Received: 3 August 2021 | Revised: 27 April 2022 | Accepted: 7 June 2022

DOI: 10.1002/jev2.12239

TECHNICAL REPORT

Ascorbate peroxidase-mediated in situ labelling of proteins in secreted exosomes

Byung Rho Lee[1] | **Tae Jin Lee**[2] | **Sekyung Oh**[3] | **Chenglong Li**[1] | **Jin-Hyuk A Song**[1] | **Brendan Marshall**[1] | **Wenbo Zhi**[2] | **Sang-Ho Kwon**[1]

[1]Department of Cellular Biology and Anatomy, Medical College of Georgia, Augusta University, Augusta, Georgia, USA

[2]Center for Biotechnology and Genomic Medicine, Medical College of Georgia, Augusta University, Augusta, Georgia, USA

[3]Department of Medical Science, Catholic Kwandong University College of Medicine, Incheon, South Korea

Correspondence
Sang-Ho Kwon, PhD, Medical College of Georgia, 1460 Laney Walker Blvd, Carl T Sanders Research & Education Building. Augusta, GA 30912, USA.
Email: kkwon@augusta.edu

Byung Rho Lee, Tae Jin Lee and Sekyung Oh contributed equally to this study.

Funding information
National Institutes of Health, Grant/Award Numbers: DK120510 (NIDDK R01), CA229370 (NCI R21)

Abstract

The extracellular vesicle exosome mediates intercellular communication by transporting macromolecules such as proteins and ribonucleic acids (RNAs). Determining cargo contents with high accuracy will help decipher the biological processes that exosomes mediate in various contexts. Existing methods for probing exosome cargo molecules rely on a prior exosome isolation procedure. Here we report an in situ labelling approach for exosome cargo identification, which bypasses the exosome isolation steps. In this methodology, a variant of the engineered ascorbate peroxidase APEX, fused to an exosome cargo protein such as CD63, is expressed specifically in exosome-generating vesicles in live cells or in secreted exosomes in the conditioned medium, to induce biotinylation of the proteins in the vicinity of the APEX variant for a short period of time. Mass spectrometry analysis of the proteins biotinylated by this approach in exosomes secreted by kidney proximal tubule-derived cells reveals that oxidative stress can cause ribosomal proteins to accumulate in an exosome subpopulation that contains the CD63-fused APEX variant.

KEYWORDS
APEX, exosomes, extracellular vesicles, oxidative stress, proximity labelling

1 | INTRODUCTION

Biological fluids such as blood and urine carry several types of extracellular vesicles, including the spherical vesicles of 40–150-nm diameter called exosomes (Shah et al., 2018). Recent studies have uncovered intercellular communication roles played by exosomes in a variety of normal and disease processes, ranging from body patterning and immune responses to tissue repair and tumour development (Bobrie et al., 2011; Lakkaraju & Rodriguez-Boulan, 2008). Packed in exosomes as cargos, select proteins and ribonucleic acids (RNAs) are thought to deliver donor cell information to recipient cells (Pastuzyn et al., 2018). Distinct cargo molecule compositions appropriate to the biological context are presumed to account for the diverse exosome-mediated responses. Better understanding of the biological roles of exosomes, therefore, requires a precise indexing of the exosome contents.

Exosomes appear to develop through a vesicle trafficking in cells. Maturation of the late endosomes into multivesicular endosomes (MVEs; also known as multivesicular bodies, MVBs) lies at the heart of exosome biogenesis (Hessvik & Llorente, 2018; Schöneberg et al., 2017). Invaginating and pinching off the limiting membrane of the late endosomes are known to generate MVEs, the interior of which is laden with intraluminal vesicles (ILVs) as a result (Hessvik & Llorente, 2018; Schöneberg et al., 2017). During the vesicle trafficking, cargo proteins and RNAs are loaded into ILVs inside MVEs (Baietti et al., 2012;

Shurtleff et al., 2016). When the MVE membrane is fused to the plasma membrane, ILVs will be secreted into the extracellular milieu as exosomes charged with a specific set of proteins and RNAs (Bebelman et al., 2020).

Several biochemical methods such as differential and density gradient centrifugations, size exclusion chromatography and polymer-mediated precipitation have been utilized to isolate exosomes (Böing et al., 2014; Jeppesen et al., 2019). Varying viscosity of biological fluids, adhesiveness of the exosome surface and variable macromolecule compositions of exosomes, however, could hinder us from preparing exosomes with consistent quality (Jeppesen et al., 2019; Momen-Heravi et al., 2012; Yuana et al., 2014). Exosome preparation through these methods typically takes long processing time and requires special equipment as well. Notably, these inherent difficulties associated with the existing exosome isolation methods might also complicate the ensuing cargo identification with inadequately discriminating exosomes from other types of extracellular vesicles.

We here take an alternative approach for exosome cargo molecule identification. We reasoned that a genetically engineered, chemical labelling of exosome cargo molecules in situ specifically either in ILVs or in secreted exosomes could bypass the exosome isolation steps. The resultant chemically modified molecules would subsequently be harvested by compatible affinity capturing. A recently developed, proximity-dependent protein biotinylation method using the engineered ascorbate peroxidase APEX could serve the purpose (Martell et al., 2012). The catalytic activity of APEX converts exogenously added biotin-phenol (also called biotinyl tyramide) in the presence of hydrogen peroxide into the highly reactive, labile biotin-phenolic radical, which in turn conjugates promiscuously to proteins in its vicinity (Martell et al., 2012). After expressing an APEX variant fused to a peptide or protein that directs a particular subcellular localization, biotinylation reaction can be induced for a short period of time, typically for around 1–2 min, and subsequently quenched, resulting in a high-confident, snapshot labelling of the proteins that exist in the subcellular location (Martell et al., 2017). The efficient, stringent affinity capturing with Streptavidin matrix following the APEX biotinylation has proven its utility in defining several subcellular-level proteomes (Lam et al., 2015).

We have thus sought to deliver an APEX variant specifically to exosomes by expressing it in the exosome biogenesis vesicle trafficking. Recent studies by others have similarly engineered either APEX (Del Olmo et al., 2019; Lobingier et al., 2017) or another promiscuous biotin ligase BirA* (Leidal et al., 2020; Rider et al., 2018), demonstrating biotinylation of extracellular vesicle-related proteins inside the cells. Our current study has thus first examined an APEX variant for the ability of specifically localizing to the exosome-generating ILVs, inducing biotinylation of the proteins that are going to be released in exosomes (intracellular labelling). We have then investigated whether the newly established exosome-targetable APEX of ours can induce proximate protein biotinylation in a cell-free condition, specifically in secreted exosomes present in the conditioned culture medium (extracellular labelling). Combining extracellular labelling with mass spectrometry analysis of the captured biotinylated proteins in secreted exosomes, we further show how oxidative stress alters exosome cargo protein contents by using a kidney proximal tubule-derived cultured cell model.

2 | MATERIALS AND METHODS

2.1 | Cell culture

HeLa (ATCC) and BUMPT (a gift from Dr. Zheng Dong, Medical College of Georgia, Augusta University) cells (Table S1) were cultured in Dulbecco's Modified Eagle's Medium (Thermo Fisher Scientific) supplemented with 5% foetal bovine serum (FBS) (Gemini), 100-U/ml penicillin, and 100-mg/ml streptomycin (Thermo Fisher Scientific) at 37°C in humidified atmosphere containing 5% CO_2. Mycoplasma contamination was examined every 4 months by using the LookOut Mycoplasma PCR detection kit (Millipore Sigma). Plasmids harbouring an APEX2 expression construct were transfected using polyethylenimine (PEI) with the DNA to PEI ratio (w/w) of 3. To establish stable cell lines, the CD63-APEX2-expressing plasmid constructed in the lentiviral vector pLX304 was packaged in HEK293T cells by using the Vira Power expression system kit (Thermo Fisher Scientific). The recipient HeLa and BUMPT cells were infected with the HEK293T cell culture medium laden with the lentiviral particles for 16 h, followed by selection with blasticidin.

2.2 | DNA constructs

DNA fragments encoding the CD63 coding sequence (CDS) with a 5′ flanked upstream open reading frame (uORF) (Ramanathan et al., 2018) and the C-terminally HA-tagged APEX2 CDS were individually PCR amplified using the Q5 High-Fidelity DNA polymerase (New England Biolabs) and subsequently assembled with the HiFi DNA assembly kit (New England Biolabs) to make the fusion cassette of uORF-CD63-APEX2-HA. Using the In-Fusion HD cloning kit (Takara), the fusion cassette as an insert was cloned into the pAAV-CMV vector (Takara). To make a lentiviral version of the CD63-APEX2-HA expression vector, DNA sequence between *NdeI* and *NheI* of pLX304 was replaced by the assembled DNA fragment encoding CD63-APEX2-HA by using the In-Fusion HD cloning kit (Takara). A version of CD63-APEX2-HA expression construct

that lacks uORF was also prepared by site-specific mutagenesis using the In-Fusion HD cloning kit. All constructs were verified by Sanger DNA sequencing analysis. Information on plasmid vectors and DNA recombination regents is summarized in Table S1.

2.3 | Exosome preparation via ultracentrifugation

In preparing exosomes via ultracentrifugation, cells were incubated with a freshly replaced serum-free medium to minimize the contamination of FBS-originated exosomes. After 30-h incubation, the conditioned medium was centrifuged at 500 × *g* for 20 min. The supernatant was then treated with 1 U/ml of Benzonase (Millipore Sigma) for 15 min at room temperature and subsequently centrifuged at 2000 × *g* for 20 min at 25°C. The resulting supernatant was further centrifuged at 10,000 × *g* for 1 h at 25°C followed by filtration through 0.2-μm asymmetric polyethersulfone (PES) membrane (Millipore Sigma). The filtered supernatant was subjected to tangential flow filtration, using the 500-kDa cutoff Biomax cassette (Millipore Sigma). The feeding rate was controlled at 4–5 ml/min, using a poly pump (Buchler) to maintain the inlet and operation pressures at <10 and <3.5 psi, respectively. Retained particles were washed with Dulbecco's phosphate buffer saline (DPBS, Thermo Fisher Scientific). The final processed sample volume was typically 10- to 15-fold concentrated. The retentate fraction containing exosomes was then centrifuged at 200,000 × *g* for 1 h at 4°C. After resuspending the pellet with DPBS, isolated extracellular vesicles containing exosomes were stored at −80°C until use.

2.4 | Nanoparticle tracking analysis

Nanoparticles in the conditioned culture medium were subjected to size and concentration measurement by either the light scattering-based Zetaview (Particle Matrix) or the tunable resistive pulse sensing-based qNano Gold (Izon). The nanopore NP150 was used in the tunable resistive pulse sensing. Before measurement, the equipment was calibrated with polystyrene reference standards to determine the optimal settings of size and concentration. Immediately before sample injection, samples were filtered through 0.2-μm nylon or PES syringes to disengage aggregated particles. Captured video clips from Zetaview were analysed by the ZetaView software 8.04.02.SP3 while current pulse signals were analysed with Izon Control Suite 3.3.2.2001.

2.5 | Intracellular labelling of exosome proteins with APEX-induced biotinylation

HeLa cells were pre-incubated with 500-μM biotin-phenol (Millipore Sigma) for 30 min and treated with 1-mM hydrogen peroxide for 1– 2 min to initiate biotinylation reaction (Martell et al., 2017) (Table S1). The biotinylation reaction was quenched by adding 10-mM sodium ascorbate, 10-mM sodium azide, and 5-mM Trolox (Martell et al., 2017).

2.6 | Extracellular labelling of exosome proteins with APEX-induced biotinylation

After culturing either HeLa or BUMPT cells in a freshly replaced 5% (v/v) FBS-containing medium for 30 h, the conditioned medium was spun at 500 × *g* for 20 min to collect the supernatant. In case of BUMPT cell experiments, cells were treated with or without 0.5-mM hydrogen peroxide (H_2O_2) for 1 h to induce oxidative stress, followed by incubating with a newly replaced medium for collecting the conditioned medium for 30 h, prior to the initial spinning of the conditioned medium. After a second centrifugation at 2000 × *g* for 20 min, the resulting supernatant was concentrated, and buffer exchanged to DPBS, using either an Amicon centrifugal concentrator (100-kDa cutoff) or a Biomax filter (500-kDa cutoff) (Millipore Sigma), depending on sample size and scale. The optimum condition for 500-μM biotin-phenol pre-incubation with the concentrated, buffer-exchanged conditioned medium (retentate fraction) was determined by comparing 4°C/16 h; 25°C/16 h; 37°C/3 h and 37°C/16 h. While all four conditions were capable of inducing APEX-dependent biotinylation, the biotin-phenol loading at 25°C for 16 h led to the most efficient labelling. Therefore, the extracellular labelling experiments for mass spectrometry analysis employed the condition of 500-μM biotin-phenol pre-incubation for 16 h at 25°C for the maximum-level labelling. the extracellular labelling for orthogonal validation, on the other hand, adopted the condition of 500-μM biotin-phenol pre-incubation for 3 h at 37°C for the convenience of the experiment. The biotin-phenol pre-incubated conditioned medium was subsequently treated with 1-mM hydrogen peroxide treatment for 1–2 min to initiate biotinylation reaction (Martell et al., 2017). The reaction was quenched by adding 10-mM sodium ascorbate, 10-mM sodium azide and 5-mM Trolox (Martell et al., 2017).

2.7 | Streptavidin affinity capturing of proteins biotinylated with extracellular labelling

Samples containing proteins biotinylated with extracellular labelling were prepared by subjecting the conditioned medium to tangential flow filtration, using the 500-kDa cutoff Biomax cassette (Millipore Sigma) with the feeding rate controlled at 4–5 ml/min, using a poly pump (Buchler) to maintain the inlet and operation pressures at <10 and <3.5 psi, respectively. The concentrated, buffer-exchanged conditioned medium (retentate fraction) was then incubated with Streptavidin beads to eliminate unconjugated biotin-phenol and non-specific biotinylated proteins. The resulting precleared retentate fraction was treated with 0.2% (w/v) SDS to permeabilize membranous particles and vesicles. Both intracellular and extracellular labelling samples were then incubated for 2 h at room temperature with Streptavidin-conjugated agarose beads (Thermo Fisher Scientific), which had been pre-blocked with bovine serum albumin (BSA) and equilibrated with 0.2% SDS in DPBS. The beads were subsequently washed extensively with 0.2% SDS and 500-mM sodium chloride. After the final washing with DPBS, the beads were boiled for 10 min with LDS sample buffer supplemented with 25-mM D-biotin to elute the biotinylated proteins. For mass spectrometry analysis, the Streptavidin beads capturing the biotinylated proteins were subjected to on-bead trypsin digestion in the Augusta University Proteomics core.

2.8 | Density gradient centrifugation

After washing with DPBS, cells were homogenized in 20-mM HEPES (pH 7.4), 1-mM EDTA, 120-mM NaCl and protease inhibitor cocktail (Thermo Fisher Scientific). The homogenate was spun at 500 × *g* for 15 min to remove unbroken cells, cell debris and nuclei. The supernatant was serially centrifuged first at 2000 × *g* for 20 min at 4°C and then at 200,000 × *g* for 1 h at 4°C. The resulting pellet was resuspended with the homogenization buffer supplemented with 10% sucrose. A continuous 10%–40% (w/w) sucrose gradient was prepared, using a gradient mixer. The resuspended pellet fraction was loaded on top of the gradient and then spun at 200,000 × *g* at 4°C for 14 h. Eleven fractions were collected, and one-tenth of each fraction was subjected to SDS-PAGE analysis.

2.9 | Western blot analysis

Cells were washed with ice-cold DPBS and then lysed in ice-cold RIPA buffer (25-mM Tris-HCl, pH 7.6, 150-mM NaCl, 0.1% SDS, 1% NP-40 and 1% sodium deoxycholate) supplemented with protease inhibitor cocktail (Thermo Fisher Scientific) on ice for 30 min. Cell lysates were spun at 10,000 × *g* for 20 min at 4°C and then sonicated. The protein concentration of the cleared lysates was measured using the BCA protein assay kit (Pierce). Fifteen micrograms of proteins per lane mixed with LDS sample buffer were run on 4%–12% Bis-Tris SDS-PAGE gel (Thermo Fisher Scientific). For exosome marker analysis, proteins from the equal volume of conditioned medium collected from either the same number of cells or the equal number of nanoparticles were run on SDS-PAGE gel. Proteins on the gel were transferred to nitrocellulose membrane and blocked with the Blocker™ BSA in PBS (Thermo Fisher Scientific) for 1 h. The membrane was then incubated with the indicated primary antibodies overnight and HRP-conjugated secondary antibodies in the blocking buffer for 1 h. We strictly followed manufactures' instructions on handling these antibodies and protocols for performing Western blot analysis (Table S1). Unsaturated chemiluminescence signals were captured and analysed by using the iBright FL1500 Imaging System (Thermo Fisher Scientific).

2.10 | Immunofluorescence microscopy

Cells were washed quickly with ice-cold DPBS containing 1-mM $CaCl_2$ and 0.5-mM $MgCl_2$, fixed with 4% paraformaldehyde (Electron Microscopy Sciences) for 20 min and blocked with 0.7% fish skin gelatin and 0.025% saponin in DPBS for more than 3 h. Primary antibodies were incubated in the blocking solution at 4°C overnight. After washed with DPBS, cells were incubated with fluorescent-conjugated secondary antibodies or Streptavidin in the blocking solution. Samples were then washed with DPBS, followed by slide mounting. We strictly followed manufactures' instructions on handling these antibodies and protocols for performing immunofluorescence microscopy (Table S1). For confocal microscopy, digital images magnified with a Plan-Apochromat 63×1.4 NA oil lens were captured with a Zeiss LSM 780 with GaAsP spectral detector. To analyse the distribution of APEX2 fusion proteins from the limiting membrane to the intraluminal space of endosomes, mCherry signal was used to define the area of interest, which represents the limiting endosome membrane. ImageJ was used to measure pixel intensities over the area defined by the mCherry signal.

2.11 | Immunogold transmission electron microscopy

Cell pellets were fixed in 4% paraformaldehyde and 0.2% glutaraldehyde in 0.1-M cacodylate buffer, pH 7.4 and processed through a graded series of ethanol (25%, 50%, 70%, 80% and 95%). After the cells were embedded in the LR White Resin (Electron Microscopy Sciences), 75-nm-thick sections were collected on 200 mesh nickel grids. Grids were baked in a 60°C oven for 5 min, floated with the section side down on drops of etching solution (5% sodium metaperiodate in PBS) for 5 min, and washed with PBS. Aldehydes were quenched for 30 min with 1-M ammonium chloride in PBS. Grids were then blocked in the Aurion Blocking Solution (Electron Microscopy Sciences) for 2 h at room temperature, floated on drops of primary antibodies diluted in the Aurion BSA-c buffer (Electron Microscopy Sciences) and incubated overnight at 4°C. Following washing in PBS, grids were floated on drops of nanogold-conjugated secondary antibodies (Nanoprobes) diluted 1:1000 in the Aurion BSA-c buffer for 2 h at room temperature. Nanogold particles were silver enhanced for 12 min using HQ Silver™ (Nanoprobes) and washed in ice-cold DI H_2O to halt enhancement. Grids were stained with 2% aqueous uranyl acetate to increase contrast and observed in a JEM 1230 transmission electron microscope (JEOL) at 110 kV. Images were acquired with an UltraScan 4000 CCD camera and a First Light Digital Camera Controller (Gatan).

2.12 | Proteinase K susceptibility

Exosome pellets were prepared as described above except that the final spin was done at 100,000 × *g* to avoid potential damaging of exosomes. The pellet was carefully resuspended in 30-mM Tris-HCl (pH 8.0) and 100-mM NaCl using pipette action with wide-bore tips. Proteinase K (New England Biolabs) was added to a final concentration of 18 μg/ml and incubated on ice for 40 min. The reaction was stopped by the addition of 5-mM PMSF (Thermo Fisher Scientific) and 2x LDS sample buffer (Thermo Fisher Scientific) supplemented with 200-mM dithiothreitol and incubated at 95°C for 10 min before SDS-PAGE analysis.

2.13 | Mass spectrometry analysis

Captured proteins were digested overnight directly on beads with sequence-grade trypsin after denaturation with 8-M urea in 50-mM Tris-HCl, pH 8.0, reduction with dithiothreitol, alkylation using iodoacetamide. Digested peptides were cleaned using a C18 spin column (Harvard Apparatus #744101) and then lyophilized. Digested peptide samples were analysed on an Orbitrap Fusion tribrid mass spectrometer (Thermo Fisher Scientific), to which an Ultimate 3000 nano-UHPLC system (Thermo Fisher Scientific) is connected. The peptide samples were first trapped on a Pepmap100 C18 peptide trap (5 μm, 0.3 × 5 mm) and then washed at 20 μl/min using 2% acetonitrile with 0.1% formic acid for 10 min. Next, the cleaned peptides were washed off the trap and further separated on a Pepman 100 RSLC C18 column (2.0 μm, 75 μm × 150 mm) at 40°C using a gradient of between 2% and 40% acetonitrile with 0.1% formic acid over 40 min at a flow rate of 300 nl/min. Eluted peptides were introduced into the mass spectrometer via nano-electrospray ionization, and the mass spectrometry analysis was performed using data-dependent acquisition in positive mode with the Orbitrap MS analyzer for precursor scans at 120,000 FWHM from 300 to 1500 m/z and the ion-trap MS analyzer for MS/MS scans at top-speed mode (3-s cycle time). Collision-induced dissociation method was used to fragment the precursor peptides with a normalized energy level of 30%. Raw MS and MS/MS spectrum for each sample were filtered and processed using the Proteome Discoverer software v1.4 (Thermo Fisher Scientific) and then submitted to SequestHT search algorithm against the Uniprot mouse database (10 ppm precursor ion mass tolerance: 10ppm, product ion mass tolerance: 0.6 Da, with static Carbamidomethylation of +57.021 Da and dynamic oxidation of methionine (+15.995 Da). Perculator PSM validator algorithm was used for peptide spectrum matching validation and false discovery rate estimation.

2.14 | Identification of biotinylated proteins and data quality assessment

The number of peptide spectrum matched (PSMs) was normalized using total PSM counts over comparison groups. The quality of datasets was evaluated, using Pearson's correlation analysis and the residual plot of PSM values. Principal component analysis (PCA) of PSM values was utilized to characterize protein expression profiles of each experimental group. Biotinylated proteins were obtained by removing proteins found in no CD63-APEX2 expression control samples as an exclusion list. The listed proteins were mapped to Entrez gene ID, using a genome-wide annotation tool for the mouse, the org.Mm.eg.db package, and enrichment analysis of the specific biotinylated proteins was then performed with linear models for microarray data, the limma package (Ritchie et al., 2015) and GO enrichment analysis, the GO summaries (Kolde & Vilo, 2015). All the analyses were performed using the R statistical language 3.6.0.

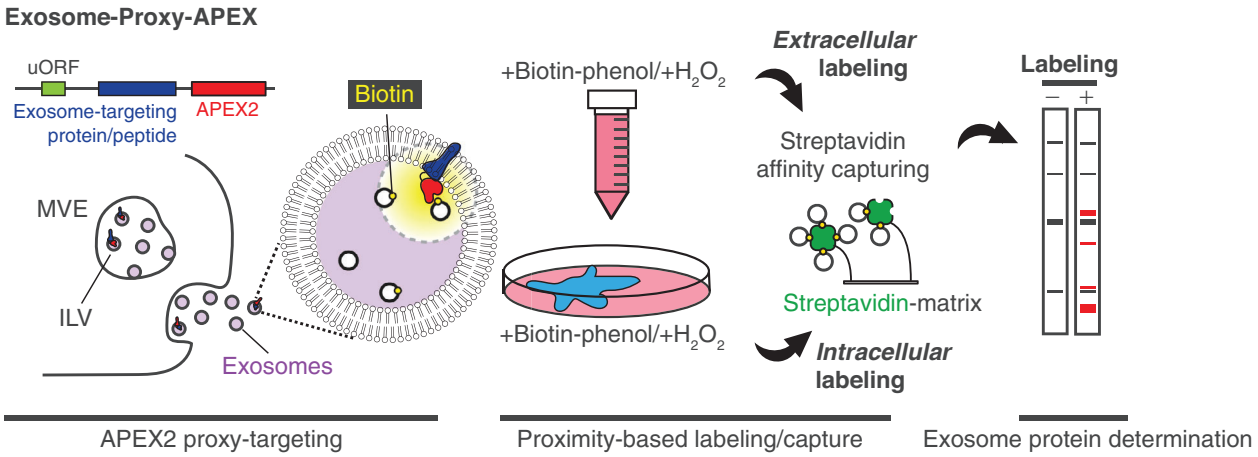

FIGURE 1 An in situ strategy for labelling exosome proteins by using the engineered ascorbate peroxidase APEX. An APEX2 variant with an annexed exosome-targeting signal is expected to localize to the key exosome biogenesis subcellular structure, namely ILVs inside MVEs, and eventually to be released in exosomes. When biotin-phenol and hydrogen peroxide are added to live cells, the APEX variant could induce biotinylation of proximate proteins specifically in ILVs (intracellular labelling). Alternatively, APEX2-mediated biotinylation could also be induced in the collected conditioned medium of the APEX-producing cell culture (extracellular labelling). The resulting biotinylated proteins would be captured with Streptavidin affinity matrix under a denaturing condition and identified with mass spectrometry analysis. The exosome-targetable APEX variants were delivered to cells by transducing either recombinant adeno-associated viral or lentiviral vectors in this study.

3 | RESULTS

3.1 | An in situ strategy for labelling exosome proteins

APEX would be able to biotinylate exosome proteins if transported to the key subcellular location in exosome biogenesis, namely ILVs within MVEs. Construction of an APEX variant with an annexed ILV localization signal would enable such localization when the fusion construct is expressed in cells. We chose the catalytically improved APEX2 variant for our study (Lam et al., 2015). Expression of an exogenous construct at a low level often helps it targeted to the desired subcellular location. We thus included an uORF (Ramanathan et al., 2018; Wethmar, 2014) in our construct to dampen the translation of the exosome-targetable APEX from the downstream main open reading frame (Figure 1). The resulting APEX catalytic activity localized in the exosome-generating subcellular structure would enable a specific labelling of exosome-related proteins in situ in response to biotin-phenol and hydrogen peroxide. We have here applied this approach of proximity-dependent labelling of exosome proteins both to live cells (Figure 1, intracellular labelling) and to the conditioned culture medium (Figure 1, extracellular labelling). Intracellular labelling would give rise to the accumulation of biotinylated proteins specifically in ILVs, which can subsequently be purified from cell lysates (Figure 1). The proteins biotinylated by intracellular labelling as well as the exosome-targetable APEX could eventually be released in exosomes. If so, the biotinylated proteins by intracellular labelling will also be purified from the conditioned medium and identified subsequently (Figure 1). On the other hand, if the catalytic activity of the exosome-targetable APEX is preserved and accessible after its release in exosomes, we would also be able to induce extracellular labelling in the collected conditioned culture medium, allowing more direct determination of the cargo protein contents of secreted exosomes (Figure 1).

3.2 | Establishing an exosome-targetable APEX variant, CD63-APEX2

We first tested whether the peptide called XPack (XP) (Yim et al., 2016) would be appropriate for establishing an exosome-targetable APEX variant. The XP peptide had previously been shown to confer the ability of exosomal secretion upon Green Fluorescence Protein (GFP) (Yim et al., 2016). We thus ligated an XP-tagged GFP amino (N)-terminally to the APEX2 coding sequence (CDS) (Figure S1a). Since GFP tends to localize to the nucleus, we also included a nucleus export signal at the C-terminus of the fusion construct to increase its expression in the cytosol (Figure S1a), where the exosome biogenesis vesicle trafficking occurs (Hessvik & Llorente, 2018; Schöneberg et al., 2017). When the resultant XP–GFP–APEX2 was expressed in HeLa cells, biotinylated proteins arose in response to biotin-phenol and hydrogen peroxide (Figure S1a, lower right), indicating that the APEX catalytic activity remains intact in this construct. We also noted that the proteins biotinylated by XP–GFP–APEX2 emerged in the conditioned medium 30 h after a pulse APEX labelling and subsequent quenching (Figure S1b). The expression of XP–GFP–APEX2 did not considerably alter the number and size of nanoparticles in the culture medium (Figure S1c).

Immunofluorescence microscopy, however, showed little endosomal localization of XP–GFP–APEX2, which instead accumulated near the cell surface (Figure S1d). XP–GFP–APEX2 did not appear to co-localize significantly with the late endosome marker LAMP2 (Figure S1d), which is en route to exosomal release and routinely used for identifying MVEs in the exosome field (Li et al., 2013). Immunogold transmission electron microscopy confirmed the limited association between XP–GFP–APEX2 and MVEs (Figure S1e). To better visualize MVEs, we expressed a constitutively active (CA) form of the small GTPase Rab5 ($Rab5^{QL}$), which is known to enlarge endosomes (Kwon et al., 2014). When analysed by confocal immunofluorescence microscopy, XP–GFP–APEX2 was less represented on the endosomal membrane than the mCherry-conjugated $Rab5^{QL}$ (Figure S1f). Since an exosome protein typically shows high-level localization in MVEs at the steady state, reflecting the MVE origin of exosomes, XP–GFP–APEX2 appears to fall short of becoming an exosome-targetable APEX variant.

Looking for an alternative means to localize APEX to exosomes, we next employed the well-characterized exosome cargo protein CD63 (Baietti et al., 2012). We made an expression construct named CD63-APEX2 by tandemly arranging the CD63 CDS, the APEX2 CDS and the HA epitope from the amino (N)- to the Carboxy (C)- termini (Figure 2a). The tetra-transmembrane protein CD63 protrudes both the N- and the C-termini to the cytosolic side and is known to maintain protein topology during exosome biogenesis (Cvjetkovic et al., 2016). ILVs are thought to form by invaginating and pinching off the limiting membrane of the late endosome, converting the cytosolic side of the late endosome membrane to the lumen side of ILVs. Thus, if targeted as desired, CD63-APEX2 would insert its four transmembrane domains into the ILV membrane; expose the N- and the C-termini to the lumen side of ILVs and induce biotinylation of the proteins in the luminal space bounded by the ILV membrane in response to biotin-phenol and hydrogen peroxide.

As expected from the use of uORF, CD63-APEX2 proteins were expressed at a much- reduced level relative to endogenous CD63, as shown by Western blot analysis with an anti-CD63 antibody (Figure 2b, anti-CD63). Western blotting with an anti-HA antibody confirmed the expression of CD63-APEX2, which migrated slower in SDS-PAGE than endogenous CD63 (Figure 2b, anti-HA). Posttranslational modifications such as glycosylation occurring during the biosynthetic secretory vesicle trafficking through the endoplasmic reticulum and the Golgi apparatus might account for the smeared resolution in SDS-PAGE of both CD63-APEX2 and endogenous CD63 (Figures 2b, 3c and S2a).

Streptavidin blotting further showed that biotinylated proteins arose from the CD63-APEX2-expressing cells after both biotin-phenol and hydrogen peroxide had been added (Figure 2c), indicating that APEX2 is catalytically intact in the fusion construct. We next examined whether the proteins biotinylated by CD63-APEX2 could be released into the culture medium. Streptavidin blotting showed that 30 h after a pulse labelling and subsequent quenching, little biotinylated proteins were left at a detectable level inside the cells (Figure 2d, cell lysates). The biotinylated proteins were instead recovered from the conditioned medium, after large particulates had centrifugally been removed as pellets (Figure 2d, 15K × *g* supernatant of serum-free (s.f.) conditioned media), indicating that most of the biotinylated proteins had been released out to the medium. Nanoparticles released from the CD63-APEX2-expressing cells displayed statistically comparable distributions in size and number to those of the control GFP-expressing cells (Figures 2e and 2f).

In contrast to XP–GFP–APEX2, CD63-APEX2 was co-localized significantly with the late endosome marker LAMP2 in confocal immunofluorescence microscopy (Figure 2g). To confirm this co-localization biochemically, cell homogenates were fractionated by density gradient centrifugation. CD63-APEX2 was co-segregated with the late-endosome marker LAMP2 (Li et al., 2013) but not with the early endosome marker EEA1 (Wilson et al., 2000) (Figure S2a). The segregation pattern of CD63-APEX2 was indistinguishable from that of endogenous CD63 (Figure S2a), which is known to travel through LAMP2-positive MVEs towards exosomal release (Poeter et al., 2014). Notably, CD63-APEX2 appears to accumulate specifically inside MVEs, as revealed by transmission electron microscopy of the cells stained with a gold-conjugated-anti-HA antibody (Figure 2h). Confocal Immunofluorescence analysis further confirmed this spatial specificity when endosomes were enlarged by expressing the CA $Rab5^{QL}$: both CD63-APEX2 and the mCherry-conjugated $Rab5^{QL}$ accumulated on the MVE membrane and its luminal space (Figure 2i). We, therefore, classify CD63-APEX2 as an exosome-targetable APEX variant.

3.3 | Intracellular biotinylation labelling of exosomal proteins with CD63-APEX2

As we noted above, CD63-APEX2 in the presence of biotin-phenol and hydrogen peroxide can induce biotinylation of proteins in cells and their subsequent release into the culture medium (Figures 2c and 2d). We thus asked whether the accumulation of CD63-APEX2 in MVEs is associated with the release of the biotinylated proteins (Figures 2c and 2d). When CD63-APEX2-expressing cells were stained with an anti-HA antibody for CD63-APEX2 and Streptavidin for biotinylated proteins, Streptavidin-positive signals, which co-localized with CD63-APEX2, emerged after biotin-phenol and hydrogen peroxide had been added together (Figure S2b), demonstrating the specificity of the APEX biotinylation. At a higher resolution with Airyscan, the CD63-APEX2 staining in endosomes appeared to surround the Streptavidin staining, presumably in the ILV lumen (Figure 2j), consistent with the proposed topology of CD63-APEX2 with the APEX2 portion protruding to the ILV lumen. The ILV membrane may limit the diffusion of the biotin-phenolic radical produced by CD63-APEX2, thereby confining protein biotinylation to the ILV interior. Of note, the Streptavidin staining appears to be sparser than that of CD63-APEX2 (Figures 2j and S2b), suggesting

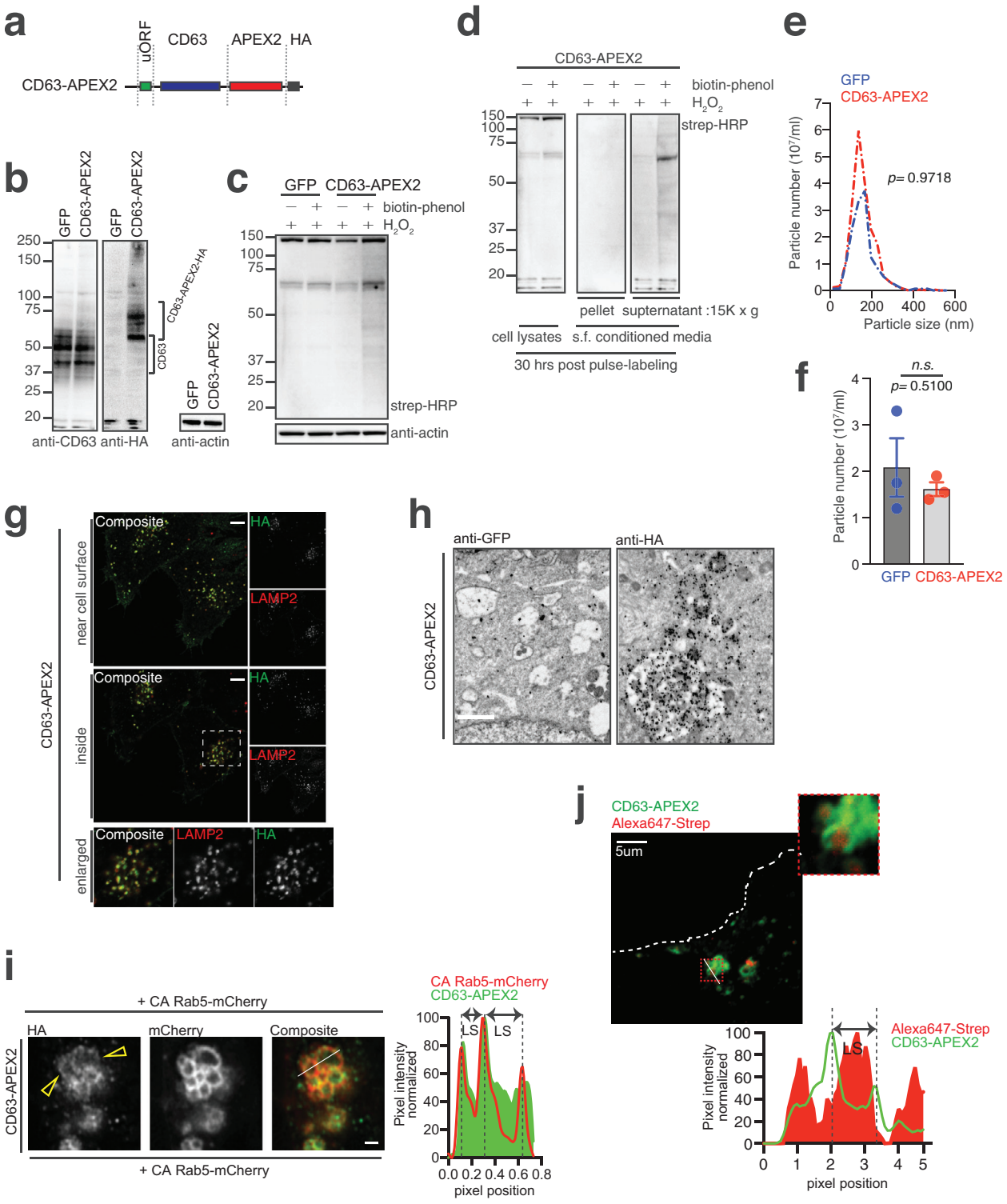

FIGURE 2 Intracellular labelling inducible by CD63-APEX2. (a) Schematic drawing of the recombinant CD63-APEX2 expression construct. uORF, upstream open reading frame to dampen translation (Ramanathan et al., 2018; Wethmar, 2014). (b) Western blot analysis for CD63-APEX2 expression as revealed by Western blot analysis with an anti-CD63 antibody (left) and an anti-HA antibody (right). Note that expression of CD63-APEX2 was lower than that of endogenous CD63 in the anti-CD63 Western blot (left) due to the use of uORF. Smeared bands of both CD63-APEX2 and endogenous CD63 might represent posttranslational modifications such as glycosylation that happen in the biosynthetic secretory pathway through the ER and Golgi apparatus. GFP, an expression control. Actin, a loading control. (c) Western blot analysis for proteins biotinylated by CD63-APEX2 in live cells. APEX biotinylation occurs in CD63-APEX2-expressing cells after biotin-phenol and hydrogen peroxide (H_2O_2) were added (+biotin-phenol, +H_2O_2). Strep-HRP, Western blotting with a horseradish peroxidase (HRP)-conjugated Streptavidin. −biotin-phenol & +H_2O_2, a mock APEX biotinylation. GFP, an expression control. Actin, a loading control. (d) Western blot analysis of biotinylated proteins in the culture conditioned medium and cell lyases after a pulse in vivo biotinylation by CD63-APEX2 and the following 30-h chase. A serum-free (s.f.) medium was used to minimize endogenous biotinylated proteins potentially present in serum. The

rather a low accessibility of either biotin-phenol or hydrogen peroxide or both across several membranous structures to the ILV interior.

The spatially restricted co-localization of CD63-APEX2 and biotinylated proteins at last demonstrates an approach of intracellular labelling of exosome proteins as proposed in Figure 1, which is inducible by the exosome-targetable APEX variant, CD63-APEX2. Streptavidin pull-down of the cell lysates containing CD63-APEX2 and its APEX-mediated biotinylation reaction products would enrich a set of proteins involved in exosome biogenesis and loaded in exosomes as cargos. Moreover, the proteins biotinylated by the intracellular labelling can also be collected by their affinity to Streptavidin from the conditioned medium after these proteins have been secreted from the cells. Thus, the intracellular labelling of exosome proteins by exosome-targetable APEX variants such as CD63-APEX2 will have broad utility.

3.4 | Extracellular biotinylation labelling of exosomal proteins with CD63-APEX2

Most APEX studies thus far have focused on the proteins in intracellular organelles. Recent studies utilizing either APEX (Del Olmo et al., 2019; Lobingier et al., 2017) or another promiscuous biotin ligase BirA* (Leidal et al., 2020; Rider et al., 2018) for extracellular vesicle studies have thus induced biotinylation inside the cells. In addition to intracellular labelling, however, APEX has also proven useful in analysing proteins existing in the synaptic cleft, an open, extracellular side of the cell surface (Cijsouw et al., 2018; Loh et al., 2016), demonstrating that the APEX methodology can be extended to studying extracellular proteins. We thus asked whether extracellular CD63-APEX2, once released in exosomes, can biotinylate proteins in situ when biotin-phenol and hydrogen peroxide are added to the conditioned medium in a cell-free manner (Figure 1, extracellular labelling). Of note, such extracellular APEX-mediated biotinylation requires that the ascorbate peroxidase activity of CD63-APEX2 be maintained after its release in exosomes and that both biotin-phenol and hydrogen peroxide be accessible to CD63-APEX2 across the exosome membrane. If so, the induction of extracellular labelling would be more direct and efficient than that of intracellular labelling as biotin-phenol and hydrogen peroxide must cross just a single lipid bilayer to initiate biotinylation inside the exosomes secreted into the conditioned medium.

Extracellular labelling would further require that the culture medium contain little endogenous peroxidase activity, which could otherwise interfere with downstream capturing and identification steps. We noted that treating a cell-free, FBS-containing medium with biotin-phenol and hydrogen peroxide generated a substantial quantity of biotinylated proteins in proportion to the added amount of FBS (Figure 3a), indicating an endogenous peroxidase activity present in FBS. A previous study indeed reported a similar activity in human serum, which would be reducible by zinc chloride via an unknown mechanism (Takahashi et al., 1987). We were likewise able to decrease to some degree the peroxidase activity from the FBS-containing medium by adding zinc chloride (Figure 3b, ZnCl). To better eliminate the endogenous peroxidase activity, we subjected the FBS-containing medium to filtration through a 500-kDa cutoff membrane. To our surprise, the peroxidase activity was predominantly partitioned into the filtrate fraction while left little in the retentate fraction (Figure 3b, compare 500-kDa filtrate and retentate), suggesting that the retentate fraction could be used for inducing extracellular labelling with CD63-APEX2 and capturing the biotinylated proteins subsequently.

We examined whether the 500-kDa retentate fraction of the conditioned medium could contain the exosome-targetable APEX variant CD63-APEX2. Western blot analysis with an anti-HA antibody revealed that CD63-APEX2 is recoverable not only from the 100,000 × *g* pellet fraction of conventional ultracentrifugation (Figure 3c, 100k × *g* pellets) but also from the 500-kDa retentate fraction of filtration (Figure 3c, 500-kDa retentate), both of which had been obtained from the conditioned medium of CD63-APEX2-expressing cells. Since previous reports showed that both the 100,000 × *g* pellet and the 500-kDa retentate fractions contain exosomes (Busatto et al., 2018; Jeppesen et al., 2014), the CD63-APEX2 proteins partitioned into the 500-kDa retentate fraction (Figure 3c) would be enclosed in exosomes. Consistently, a substantial quantity of known exosome cargo proteins such as ALIX, Flotillin 1 and SDCBP (Ghossoub et al., 2014) was recovered from the 500-kDa retentate fraction, while these proteins

conditioned medium was spun at 15,000 × *g* (15k × *g*) to pellet down large particulates. (e) Nanoparticle tracking analysis of the medium of cells expressing CD63-APEX2 or the control GFP. The Kolmogorov–Smirnov test did not detect a noticeable difference between the two groups. (f) Multiple measurements of particle numbers by nanoparticle tracking analysis of the medium of cells expressing CD63-APEX2 or the control GFP. The Kolmogorov–Smirnov test did not detect a noticeable difference between the two groups. (g) Confocal immunofluorescence micrographs of CD63-APEX2-expressing cells show endosome localization of CD63-APEX2 as revealed by staining with an anti-HA antibody. LAMP2, an endosome marker. Scale bar, 5 μm. (h) Transmission electron micrographs of CD63-APEX2-expressing cells labelled with a gold-conjugated anti-GFP (left, a control for background) and anti-HA (right, CD63-APEX2) antibodies. Scale bar, 1 μm. (i) Confocal immunofluorescence micrographs of the endosomes expressing an mCherry-fused constitutively active form of Rab5 (CA Rab5-mCherry). Signal intensities along the white line connecting two endosomes (yellow open arrowheads) in a deconvoluted image were quantified (right). LS, the lumenal space of endosomes. Scale bar, 1 μm. (j) Confocal immunofluorescence micrographs of CD63-APEX2-expressing cells after APEX biotinylation induction. Cells were fixed 30 min after the biotinylation induction and quenching to allow diffusion of biotinylated proteins. CD63-APEX2, green (Alexa 488). Biotinylated proteins, red (Alexa 647-Strep). The dotted red rectangle in the lower left micrograph was enlarged to the upper right. Signal intensities along the white line in the lower left micrograph were quantified in the right plot. LS, the lumenal space of endosomes. Scale bar, 5 μm

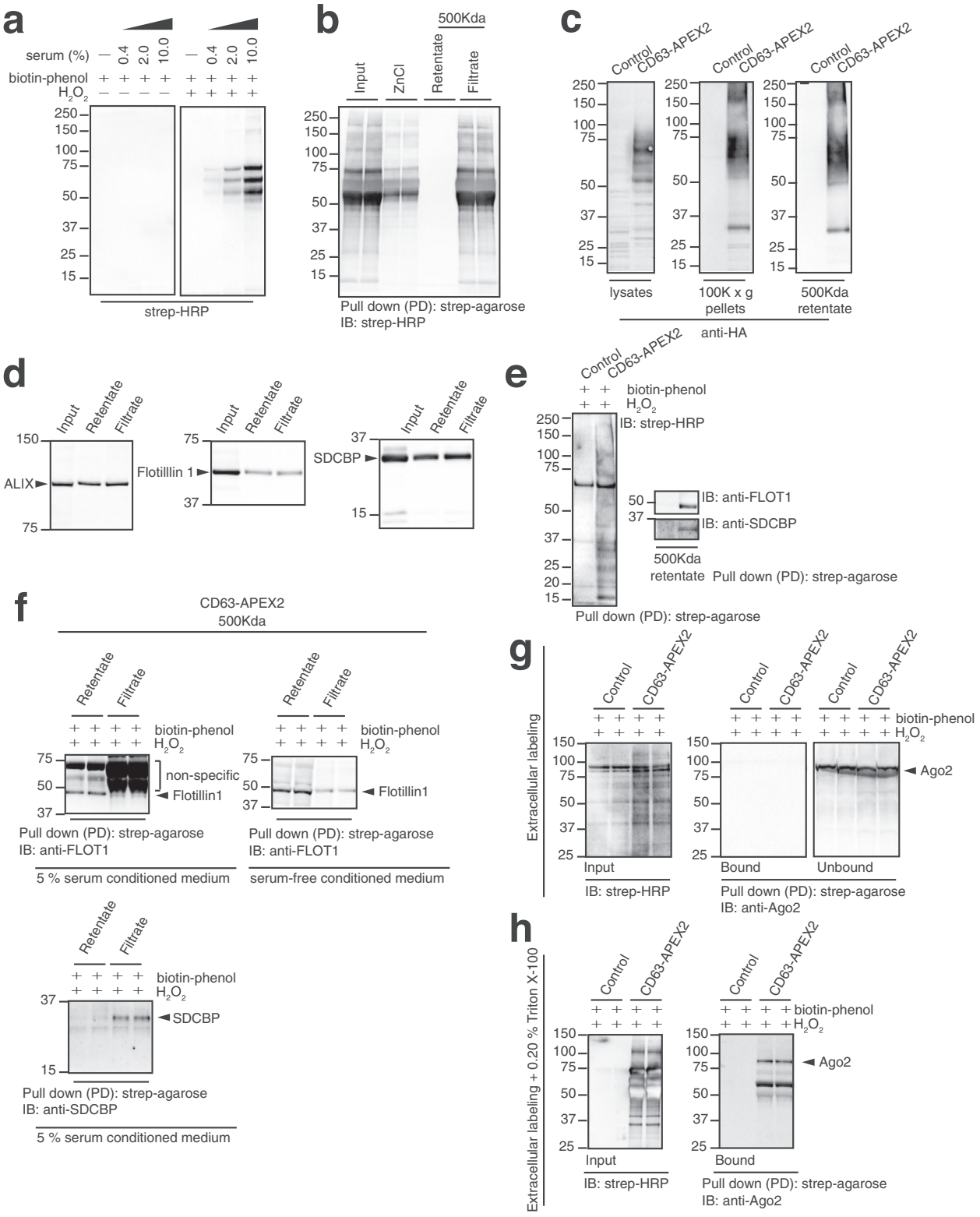

FIGURE 3 Extracellular labelling inducible by CD63-APEX2. (a) Western blot analysis of cell-free media supplemented with a titration series of FBS. Strep-HRP, Western blotting with an HRP-conjugated Streptavidin. Note that Streptavidin-reactive biotinylated proteins emerge in response to biotin-phenol and H_2O_2. (b) Western blot analysis of proteins captured by Streptavidin-conjugated agarose resin (PD: Strep-agarose) to detect Streptavidin-reactive biotinylated proteins (IB: Strep-HRP) induced by biotin-phenol and H_2O_2 in FBS. Medium containing 4% (v/v) FBS was either treated with 5-mM ZnCl or filtered through a 500-kDa cutoff membrane. Note biotinylated proteins were predominantly fractionated into the filtrate fraction while an undetectable level left in the retained material (Retentate). (c) Western blot analysis to detect CD63-APEX2 (anti-HA) in cell lysates and in the conditioned medium of cells expressing either CD63-APEX2 or the GFP control. 100k × *g* pellet, pelleted material in the conditioned medium after 100,000 × *g* centrifugation. 500-kDa

also exist in the filtrate fraction of the conditioned medium (Figure 3d), warranting the use of the 500-kDa retentate fraction in inducing extracellular biotinylation labelling of exosome proteins with CD63-APEX2.

Adding biotin-phenol and hydrogen peroxide to the 500-kDa retentate fraction induced biotinylation of a wide mass range of proteins (Figure 3e, IB: strep-HRP), demonstrating an approach of extracellular biotinylation labelling inducible by the exosome-targetable APEX variant CD63-APEX2 with coupled filtration. The biotinylated proteins in the 500-kDa retentate fraction contained known exosome cargo proteins such as Flotilin-1 and SDCBP (Ghossoub et al., 2014) as shown by Western blot analysis of Streptavidin-captured materials (Figures 3e and 3f). Of note, the biotinylated Flotilin-1 and SDCBP proteins were recovered not only from the 500-kDa retentate fraction but also from the filtrate fraction, which would have a high level of background biotinylation caused by FBS as shown above (Figures 3a and 3b). This observation suggests either that a subset of extracellular CD63-APEX2 be present in the filtrate fraction or that Flotilin-1 and SDCBP be biotinylated by the peroxidase activity present in FBS rather than by CD63-APEX2. Whereas the biotinylated SDCBP proteins were mostly recovered from the filtrate fraction, biotinylated Flotilin-1 proteins were retrieved largely from the retentate fraction (Figure 3f, left and bottom), representing uneven biotinylation profiles induced by CD63-APEX2 in the 500-kDa retentate and the filtrate fractions.

We further demonstrated that the extracellular labelling by CD63-APEX2 can be induced in a serum-free conditioned medium, as revealed by Western blot analysis of Streptavidin-captured, biotinylated Flotillin-1 proteins, which again displayed disproportionate partitioning into the 500-kDa retentate fraction (Figure 3f, right). Since our extracellular labelling procedure incubates cells in the collecting medium for a long period of time (i.e., 30 h; see Materials and Methods), however, the biotinylation profile obtained from the serum-free conditioned medium might report unwanted physiological alterations of the cultured cells. Therefore, we henceforth focused on analysing the conditioned culture medium that contained FBS, which would be subjected to filtration to reduce the FBS-inherent background biotinylation before inducing biotinylation.

A component of the RNA-induced silencing complex, Ago2 is known to be secreted via an unclear mechanism (Jeppesen et al., 2019; Melo et al., 2014). We were not able to capture Ago2 with Streptavidin matrix as a protein biotinylated by extracellular labelling with CD63-APEX2 in the 500-kDa retentate fraction of the conditioned medium of CD63-APEX2-expressing cells (Figure 3g, the Bound blot of Strep agarose pull down), suggesting that Ago2 be either unreactive to the biotin-phenolic radical or absent in the CD63-APEX2-containing exosomes. On the other hand, the conditioned medium per se contained a substantial quantity of Ago2 proteins, as revealed by Western blot analysis of the proteins that had not been captured by Streptavidin matrix (Figure 3g, the Unbound blot of Strep agarose pull down). Detergent addition to the conditioned medium followed by extracellular labelling induction, however, caused Ago2 to be biotinylated (Figure 3h, the Bound blot of Strep agarose pull down). CD63-APEX2 released from the exosomes that had been dissolved in response to the added detergent might account for the Ago2 biotinylation. These results suggest that Ago2 be secreted into the cell culture medium via a mechanism other than the release in the CD63-APEX2-containing exosomes.

To summarize, the retrieval of SDCBP and Flotilin-1 (Figures 3e and 3f) but not Ago2 in the absence of added detergent (Figures 3g and 3h) from the Streptavidin-captured proteins demonstrate that extracellular labelling can be induced specifically in the interior of the membrane-bound, CD63-APEX2-containing exosomes, rather than non-specifically in the conditioned culture medium. We noted that XP–GFP–APEX2-expressing cells also produced Streptavidin-reactive biotinylated proteins in the conditioned medium in response to biotin-phenol and hydrogen peroxide (Figure S3). However, these biotinylated proteins did not include a detectable level of Flotilin-1 and SDCBP (Figure S3), again ruling out the use of XP–GFP–APEX2 as an exosome-targetable APEX variant.

3.5 | Protein content indexing of the CD63-APEX2-containing exosomes derived from the conditioned medium of mouse proximal tubule-derived cells

We next applied the CD63-APEX2-induced extracellular labelling strategy to indexing exosome protein contents through mass spectrometry analysis of the biotinylated proteins. In doing so, we further sought to extend our extracellular labelling

retentate, 500-kDa filter-retained material of the conditioned medium. (d) Western blot analysis of the 500-kDa filtrated (filtrate) and infiltrated (retentate) fractions of the conditioned medium for the known exosome marker proteins, ALIX (left), Flotillin-1 (middle), and SDCBP (right). (e) Western blot analysis of the proteins biotinylated in response to biotin-phenol and H_2O_2 in the 500-kDa infiltrated material (500-kDa retentate) of the conditioned medium of cells expressing either CD63-APEX2 or the GFP control, demonstrating an extracellular labelling inducible by CD63-APEX2. Biotinylated proteins were captured with Streptavidin agarose matrix (PD) and then subjected to Western blot analysis (IB) with the indicated antibodies. (f) Western blot analysis of biotinylated exosome cargo proteins in the filter-fractionated conditioned medium of CD63-APEX2-expressing cells. Cells were incubated either in a 5% (v/v) FBS-containing medium (left and bottom) or in a serum-free medium (right) for 30 h. The conditioned medium was then filtered through 500-kDa cutoff membrane. The filtrate and retentate fractions were subsequently treated with biotin-phenol and H_2O_2. Biotinylated proteins were captured with Streptavidin agarose matrix (PD) and then subjected to western analysis (IB) with the indicated antibodies. (g and h) Western blot analysis to examine the presence of Ago2 in the biotinylated proteins induced by extracellular labelling of the 500-kDa-retentate conditioned medium fraction. (g) Bound: proteins pull-downed by Streptavidin agarose matrix. Unbound: proteins not pull-downed by Streptavidin agarose matrix. (h) 0.2% (v/v) Triton X-100 was added to the conditioned medium before inducing extracellular labelling to release CD63-APEX2 from extracellular vesicles.

methodology established above in HeLa cells to another cell line and to a physiological setting as well. The kidney proximal tubules are known to be exposed to a variety of oxidative insults (Chevalier, 2016; Ratliff et al., 2016). We, therefore, chose the mouse kidney proximal tubule-originated BUMPT cells (Ma et al., 2020) to stably express CD63-APEX2. Three independent lines each of the control parental BUMPT cells and CD63-APEX2-expressing cells were either treated with 0.5-mM hydrogen peroxide (H_2O_2) for 1 h to induce oxidative stress or left untreated, followed by incubation of the cells with newly replaced culture media that lacked hydrogen peroxide for the following 30 h (Figure 4a). Extracellular labelling was then induced in the 500-kDa retentate fractions of the collected conditioned media. The resulting biotinylated proteins captured on the Streptavidin matrix were released as peptides by on-bead trypsin digestion. Subsequent mass spectrometry analysis called the proteins specifically biotinylated by CD63-APEX2 after excluding those also found in the control groups (Table S2a).

We noted that levels of biotinylation, as revealed by distributions of peptide-to-spectrum matched (PSM), were comparable not only among the replicates of a given treatment but also regardless of the oxidative stress treatment (Figure S4a). However, the extracellular labelling of the stressed cell medium showed less species of biotinylated proteins than that of the unstressed cell medium (Figure S4b), indicating that the oxidative stress somehow reduced the number of the protein species biotinylated by CD63-APEX2. We noted that the proteins identified by the CD63-APEX2-induced extracellular labelling approach showed a high-degree correlation when any two biological replicates of a given treatment were compared (Figure S4c), demonstrating the reproducibility and robustness of our mass spectrometry approach in combination with the CD63-APEX2-induced extracellular labelling.

Analysis of the BUMPT cell data identified a high-confident set of 287 proteins, which shared 56 proteins with the set of the top 100 proteins in the Exocarta database (Keerthikumar et al., 2016) (Figure S4d). The remainder 44 proteins in the top 100 protein set of the Exocarta database were not detected in our method, however. The CD63-APEX2-induced extracellular labelling dataset, on the other hand, contained 231 proteins that were absent in the Exocarta top 100 protein set (Figure S4d and Table S2b). Different cell origins and varying mass spectrometry data depths between our dataset and the Exocarta dataset might account for the limited overlap between the two protein sets. Of note, since the CD63-induced extracellular labelling can induce biotinylation in a CD63-APEX2-containing subpopulation of exosomes present in the 500-kDa retentate fraction, the 44 proteins recovered only from the Exocarta top 100 protein set might represent such proteins as could be contained in the other exosome subpopulations.

Comparisons between the stressed and the unstressed BUMPT cell data gave rise to lesser correlation values than those between biological replicates of the same treatment (Figure S4c), suggesting that specific sets of proteins be enriched per each treatment group. Indeed, fold change analysis revealed proteins that were differentially enriched in the stressed and the unstressed cell groups (Figure 4b and Table S2c). Thbs1 and Hsp90, for example, were recovered more from the conditioned medium of the unstressed cells (Figure 4b and Table S2c), which were confirmed by two independent orthogonal extracellular labelling experiments (Figure 4d).

The proteins uniquely identified from the stressed cell medium included various components of both the large and small subunits of the ribosome, including Rps6, Rpl13, Rps9, Rpl19 and so on (Figure 4b and Table S2c). Consistent with this result, functional enrichment analysis of the stressed cell dataset revealed that protein production-related gene ontology (GO) terms (Ashburner et al., 2000) ranked high among those of various biological processes and molecular functions (Figure 4c, up-regulated and Table S2d). Two independent orthogonal extracellular labelling experiments confirmed the specific enrichment of the ribosomal small subunit protein Rps6 in the conditioned medium of the stressed cells (Figure 4d).

A recent study showed that conditioned culture media of various cell types contain extracellular vesicle-free ribosomes (Tosar et al., 2020). We thus examined whether Rps6 and other ribosomal proteins could be co-purifying, non-exosomal bystander proteins. Consistent with the above extracellular labelling data (Figure 4b–d and Table S2), exosomes prepared by the conventional ultracentrifugation method also contained Rps6, the level of which increased in response to oxidative stress (Figure 4e, left). Proteinase K treatment of the isolated exosomes slightly lowered the level of Rps6 from both the stressed and the unstressed cell exosomes, while leaving the majority of Rps6 protein unaffected (Figure 4e, left). The Proteinase K catalysis in our assay condition appeared to be active, as shown by the efficient hydrolysis of the control substrate BSA (Figure 4e, right). Thus, while extracellular Rps6 and other ribosomal components can exist to some extent unbounded by vesicles as shown previously (Tosar et al., 2020), a substantial share of these proteins appears bounded by vesicles, which shield their interior from proteolysis by Proteinase K. Moreover, supporting our observation using the CD63-APEX2-induced extracellular labelling (Figure 4b–d and Table S2), the ultracentrifugation-mediated exosome preparation also shows that the level of the ribosomal protein Rps6 in exosomes increases in response to oxidative stress contained (Figure 4e).

To conclude, we have demonstrated that the CD63-APEX2-induced extracellular labelling in combination with mass spectrometry can define a reliable set of proteins released in the exosomes that harbour CD63-APEX2. We have further shown that the CD63-APEX2-induced extracellular labelling can be executed in diverse cell types and physiological settings, indicating the broad utility of our approach. Our data also revealed that kidney proximal tubule-derived cells can accumulate ribosomal proteins in exosomes in response to oxidative stress, suggesting that these proteins in exosomes may either report on cellular oxidative stress or mediate an appropriate intercellular communication.

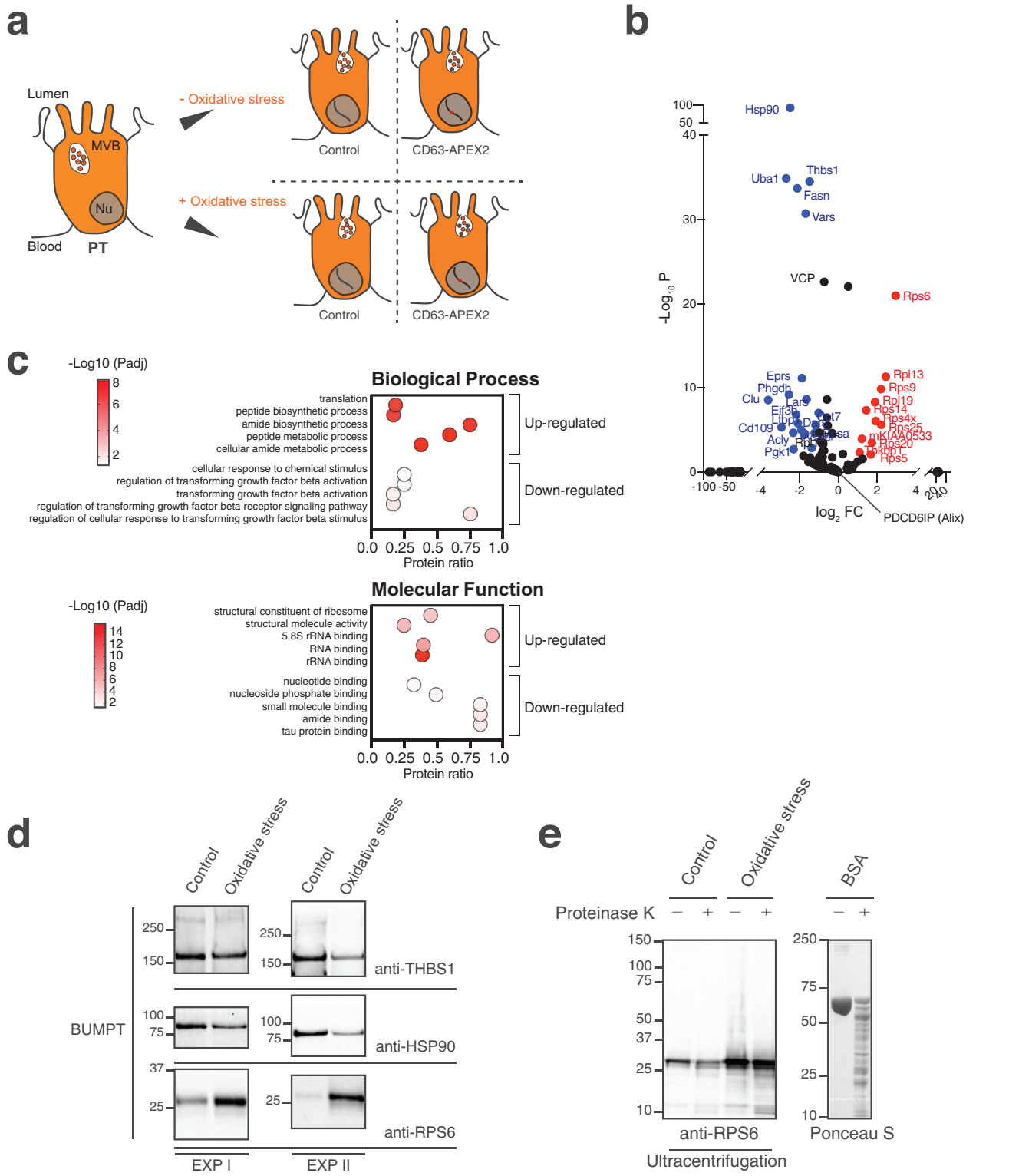

FIGURE 4 Indexing of protein contents of the CD63-APEX2-containing exosomes in BUMPT cells in response to oxidative stress. (a) Experimental schemes showing BUMPT cells of the mouse kidney proximal tubule origin and oxidative stress treatment. Extracellular labelling was induced in the 500-kDa-retentate fraction of conditioned media of BUMPT cells stably expressing CD63-APEX2 and control cells after having treated the cells with 0.5-mM H_2O_2 for 1 h (+oxidative stress) or not (−oxidative stress). Biotinylated proteins were captured by Streptavidin affinity matrix from three biological replicates of each treatment group and subsequently analysed by mass spectrometry. (b) A volcano plot showing the distribution of identified proteins by fold change (FC, +oxidative stress/−oxidative stress, *x* axis) and *p* value (*y* axis). Each dot represents individual protein species. Red, protein species enriched by oxidative stress treatment replicates. Blue, protein species enriched in no oxidative stress treatment replicates. (c) Functional enrichment analysis of the oxidative stress

4 | DISCUSSION

Existing methods for probing exosome contents rely on a prior exosome isolation procedure, which utilizes biophysical properties of exosomes (Jeppesen et al., 2019; Momen-Heravi et al., 2012; Yuana et al., 2014). These isolation methods fractionate various extracellular vesicles by density, shapes or surface charges and monitor such fractions that harbour select molecules known to co-segregate with exosomes (Jeppesen et al., 2019; Momen-Heravi et al., 2012; Yuana et al., 2014). These methods usually employ such equipment as ultracentrifuges and liquid chromatography systems. Recent studies have uncovered a growing list of novel classes of extracellular vesicles and subclasses of exosomes as well (Jeppesen et al., 2019; Zhang & Schekman, 2013; Zhang et al., 2018). Accordingly, the resolution of the existing methods might not suffice to delineate and discern all these heterogeneous vesicle types, and the ensuing cargo identification steps could unveil ambiguous, non-selective lists of exosome constituents.

Our alternative in situ labelling approach using APEX-dependent proximate protein biotinylation to determine exosome contents bypasses the requirement of exosome isolation. Targeted expression of the APEX variant CD63-APEX2 either in exosome-generating ILVs in live cells (intracellular labelling) or in secreted exosomes in the conditioned culture medium (extracellular labelling) is the prerequisite for executing this in situ labelling. Proximate protein biotinylation can then be induced inside the CD63-APEX2-residing vesicles by treating hydrogen peroxide for a short period of time (1–2 min) in the presence of biotin-phenol, enabling a subpopulation-level exosome cargo labelling and subsequent identification.

Several attempts have recently been made to utilize proximity labelling proteomics to profile exosome protein contents by inducing protein biotinylation in live cells, including studies using APEX2-fused RAB (Del Olmo et al., 2019) and GPCR (Lobingier et al., 2017); and BirA*-fused LMP1 (Rider et al., 2018) and LC3 (Leidal et al., 2020). Our intracellular labelling approach using CD63-APEX2 adds a dimension to the repertoire of toolkits for labelling exosome proteins in live cells. These multiple live intracellular labelling methods will lead us to a better understanding of how various, ever-growing classes of extracellular vesicles are made in cells and how specific, distinct sets of cargo molecules are loaded into each type of these vesicles.

In developing such a means for labelling exosomal proteins with covalent biotin adducts, one should carefully characterize the intracellular trafficking trajectory and the subsequent exosomal release of the protein or peptide variant fused to either APEX or BirA*. Moreover, the profiles of the resultant biotinylated proteins should be meticulously examined whether these contain previously known exosomal proteins. We initiated our study by utilizing the peptide called XPack (XP) (Yim et al., 2016) to establish an exosome-targetable APEX variant. However, we ruled out the use of the XP-fused APEX variant by finding that it did neither traffic along the secretory pathway towards exosomal release (Figure S1) nor biotinylate known exosomal proteins (Figure S3). Using the same principle, however, we established that another APEX variant, CD63-APEX2 fulfils the requirements to be an exosome-targetable APEX variant (Figures 2 and S2), representing a prototypical development of exosomal protein biotinylation.

A crucial addition by our current study to the exosome protein profiling field should be the development of the "extracellular labelling" approach for elucidating exosome contents. In our CD63-APEX2-induced extracellular labelling, the conditioned medium of the cells expressing CD63-APEX2 is collected and processed to remove an unwanted endogenous peroxidase activity through simple filtration (Figure 3). The resulting materials will subsequently be subjected to APEX biotinylation, leading to labelling of proteins in the vesicles in which the catalytically active CD63-APEX2 resides (Figure 3). This extracellular labelling procedure is to be executed without separating exosomes out of the complex extracellular vesicle and particle population. Moreover, our extracellular labelling strategy with CD63-APEX2 could complement shortcomings of other exosome profiling methodologies. For example, the CD63-APEX2 approach could circumvent the difficulty frequently encountered in using exosome-capturing antibodies, for biological fluids contain numerous substances that interfere with antibody–antigen interaction, such as massive levels of immunoglobulins and albumin in serum.

In setting up the CD63-APEX2-induced extracellular labelling, potential complications from contaminating cells and medium-originated components other than the CD63-APEX2-harbouring exosomes were carefully minimized. That is, (1) unbroken cells in the conditioned medium were removed by centrifugation and filtration; and (2) unreacted biotin-phenol and non-specific biotinylated proteins remaining in the medium were precleared with Streptavidin matrix before lysing the vesicles

cell dataset revealing that protein production-related gene ontology (GO) terms (Ashburner et al., 2000) rank high among various biological processes and molecular functions. (d) Western blot analysis of select proteins identified by CD63-APEX2-mediated extracellular labelling in BUMPT cells with (oxidative stress) or without (Control) oxidative stress treatment. Note that while Thbs1 and Hsp90 were more enriched in the samples obtained without oxidative stress, the ribosomal component Rps6 is recovered more from oxidative stress-treated samples. Results of two independent experiments are presented. (e) (Left) Western blot analysis of Rps6 in exosomes isolated by the conventional ultracentrifugation method from the conditioned medium of BUMPT cells. The media were subjected to Proteinase K digestion before the Western blot analysis. Note that Rps6 was recovered more from the medium of oxidative stress-treated cells (oxidative stress) than that of untreated cells (Control). Proteinase K treatment slightly decreased the level of Rps6, suggesting that the majority of Rps6 is enclosed in Proteinase K-inaccessible structures such as exosomes. (Right) Ponceau S staining of SDS-PAGE-resolved bovine serum albumin (BSA) on nitrocellulose membrane with or without prior Proteinase K digestion. Note degradation products of BSA (+Proteinase K), demonstrating that Proteinase K is enzymatically active.

(see Materials and Methods). Moreover, spatial specificity of biotinylation by the CD63-APEX2-induced extracellular labelling was also confirmed. For example, when extracellular vesicles had been lysed before inducing the APEX biotinylation, CD63-APEX2 became able to biotinylate Ago2, which would otherwise remain unbiotinylated (Figures 3g and 3f), indicating that the catalytic activity of CD63-APEX2 is confined to the interior of the exosomes.

We have demonstrated that mass spectrometry analysis following Streptavidin affinity capturing of the proteins biotinylated by the CD63-APEX2-induced extracellular labelling can identify a reliable set of proteins secreted together with CD63-APEX2 in exosomes (Figures 4, S4 and Table S2). In doing so, we have shown that the CD63-APEX2-induced extracellular labelling approach, initially developed in HeLa cells (Figure 3), can be applied to another cell line, namely the mouse kidney proximal tubule-derived BUMPT cells (Figures 4, S4 and Table S2), implying that this methodology can be applied to any cell type. We identified a set of 287 proteins from the CD63-APEX2-induced extracellular labelling of the conditioned medium of BUMPT cells (Figures 4, S4 and Table S2). These 287 proteins may constitute a parsimonious set of proteins present in an exosome subpopulation, in which CD63-APEX2 also resides. Fifty-six out of the 287 proteins were also found in the Exocarta database top 100 protein set, which had been defined from multiple types of cells and biological fluids; under various physiological conditions; and through a variety of conventional exosome isolation methods (Figure S4d and Table S2b). Forty-four proteins in the Exocarta database top 100 protein set were not recovered in the protein set of the CD63-APEX2-induced extracellular labelling. These 44 proteins might include such constituents as could be housed in exosome subpopulations other than the CD63-APEX2-containing one; and as could be identified under other physiological settings (Figure S4d and Table S2b). On the other hand, the 231 (287 minus 56) proteins recovered only from the CD63-APEX2-induced extracellular labelling of the BUMPT cell medium might include proteins pertaining to the physiology of the kidney proximal tubule as well as those existing in the CD63-APEX2-containing exosome subpopulation (Figure S4d and Table S2b).

Since the kidney proximal tubule is often exposed to oxidative insults (Chevalier, 2016; Ratliff et al., 2016), we performed the CD63-APEX2-induced extracellular labelling of exosome proteins in BUMPT cells that had received oxidative stress or not (Figures 4 and S4). Mass spectrometry analysis of the biotinylated proteins revealed a specific alteration in exosome protein contents induced by oxidative stress. Most strikingly, we noted that cells that had received oxidative stress specifically accumulated components of both the ribosomal large and small subunit components as a distinguished molecular class in secreted exosomes (Figures 4b–e, S4d and Table S2). Whether these ribosomal proteins secreted in exosomes relay donor cell information to the recipient cells, or they just play a role as stress biomarkers on exosomes remains as a subject to study further.

Although APEX promiscuously biotinylates proximate proteins and Streptavidin affinity matrix efficiently captures the resultant biotinylated proteins (Lam et al., 2015), an APEX approach, in general, may only incomprehensively reveal constituents of a target proteome. The highly reactive, labile biotin-phenolic radical, which is converted from biotin-phenol in response to hydrogen peroxide (Martell et al., 2012) is thought to conjugate to proximate proteins through chemically permissive, electron-rich amino acid side chains (Martell et al., 2017). Thus, not all the proteins available in the vicinity of a given APEX protein such as CD63-APEX2 could be biotinylated. Moreover, the optimum biotin-phenol pre-incubation condition should be determined empirically as the extent of its diffusion across various biological membranes likely varies depending on the experimental system. After testing several conditions, our current CD63-APEX2-induced extracellular labelling approach chose to pre-incubate the filter-retained conditioned media (the 500-kDa retentate fraction) with 500-μM biotin-phenol at 25°C for 16 h, followed by treatment with hydrogen peroxide for 1–2 min, which in our system produced the highest level of biotinylation (see Materials and Methods). While this condition worked in the current study, there may remain a room to improve further to reach a greater coverage in identifying proteins released in the CD63-APEX2-containing exosomes. Therefore, these inherent properties of the APEX method may introduce a considerable bias in the make-up of the protein list identified by the CD63-APEX2-mediated extracellular labelling. However, our CD63-APEX2-induced extracellular labelling approach may have merits in analysing constituents of an exosome subpopulation, while validating results of various, complementary exosome profiling methods.

Notably, to induce "extracellular" labelling with CD63-APEX2, the APEX substrate biotin-phenol must cross just a single lipid bilayer to induce biotinylation in the CD63-APEX2-harbouring exosomes present in the conditioned medium. By contrast, "intracellular" labelling with CD63-APEX2 requires the APEX substrate to diffuse through multiple membranous structures to reach the interior of the ILVs, in which CD63-APEX2 is localized before its secretion into exosomes. We indeed observed that the labelling efficiency of extracellular labelling is superior to that of intracellular labelling, the former requiring lesser amount of cell culture than the latter to achieve a comparable level of biotinylation by CD63-APEX2. The issue of labelling efficiency aside, the two labelling approaches with CD63-APEX2 may provide us with distinct opportunities for identifying exosome-relevant factors. That is, extracellular labelling with CD63-APEX2 likely identifies, for the most part, proteins that have been secreted into the interior of exosomes as cargos. On the other hand, we envision that intracellular labelling with CD63-APEX2 may also uncover proteins that are involved in exosome biogenesis and other exosome-pertinent intracellular procedures, in addition to those that are going to be released as exosome cargos.

We speculate that our APEX-induced exosome protein labelling approach can trace the dynamics of exosome content compositions over time. Importantly, the APEX-induced exosome protein labelling can take snapshots of exosome contents in a

temporal sequence in response to a certain treatment. Moreover, the APEX-induced exosome protein labelling would allow us to compare exosome contents from different cell types using a chosen exosome-targetable APEX variant such as CD63-APEX2, which would explain how much cell origins of exosomes influence the molecular makeups of exosomes. Likewise, an exosome-targetable APEX variant can also be expressed in a subset of the culture to label exosome components secreted specifically from the APEX-expressing cells, enabling finer analysis of the exosome-mediated intercellular interaction in a heterogenous cell population. Moreover, developing and characterizing additional APEX variants would lead us to better appreciate the heterogeneity of the population of exosomes and other extracellular vesicles secreted from a given cell type or tissue. Since APEX has recently been shown to label not only proximate proteins but also RNAs (Fazal et al., 2019), our approach could further be extended to analysing the exosome RNA contents, which are presumed to be equally important as the protein contents in exosome biology. Finally, future studies would be able to utilize an animal model for APEX-induced labelling of exosome contents. We would benefit from such an animal model to discover better biomarkers with advanced information on kinetics and cell origins.

ACKNOWLEDGEMENTS

We thank the CBA Electron Microscopy and Histology core for excellent assistance with ultrastructure. We also thank Dr. Zheng Dong at the Department of Cellular Biology and Anatomy, Medical College of Georgia, Augusta University for providing us with the BUMPT cell line derived from the mouse kidney proximal tubule. This work was supported by the National Institutes of Health grants DK120510 (NIDDK R01) and CA229370 (NCI R21) to Sang-Ho Kwon.

CONFLICT OF INTEREST

The authors declare no competing interests.

AUTHOR CONTRIBUTIONS

Executed experiments: Byung R. Lee, Tae J. Lee, Sekyung Oh, Chenglong Li, Jin-Hyuk A. Song, Brendan Marshall, Wenbo Zhi and Sang-Ho Kwon. *Wrote the manuscript*: Byung R. Lee, Tae J. Lee, Sekyung Oh, Brendan Marshall, Wenbo Zhi and Sang-Ho Kwon. *Designed and supervised the project*: Sang-Ho Kwon. *Obtained funding*: Sang-Ho Kwon. *Discussed and analysed the data*: Byung R. Lee, Tae J. Lee, Sekyung Oh, Chenglong Li, Jin-Hyuk A. Song, Brendan Marshall, Wenbo Zhi and Sang-Ho Kwon. All authors read and approved the final manuscript.

DATA AVAILABILITY STATEMENT

The authors declare that the data supporting the findings of this study are available within the paper and its supplementary information files. The proteomics data of this study have also been deposited to the ProteomeXchange Consortium (www.proteomexchange.org) with the project accession number PXD025852.

ORCID

Sekyung Oh https://orcid.org/0000-0002-6880-5281
Sang-Ho Kwon https://orcid.org/0000-0001-9074-4641

REFERENCES

Ashburner, M., Ball, C. A., Blake, J. A., Botstein, D., Butler, H., Cherry, J. M., Davis, A. P., Dolinski, K., Dwight, S. S., Eppig, J. T., Harris, M. A., Hill, D. P., Issel-Tarver, L., Kasarskis, A., Lewis, S., Matese, J. C., Richardson, J. E., Ringwald, M., Rubin, G. M., & Sherlock, G. (2000). Gene ontology: Tool for the unification of biology. The Gene Ontology Consortium. *Nature Genetics*, *25*, 25–29.

Baietti, M. F., Zhang, Z., Mortier, E., Melchior, A., Degeest, G., Geeraerts, A., Ivarsson, Y., Depoortere, F., Coomans, C., Vermeiren, E., Zimmermann, P., & David, G. (2012). Syndecan–syntenin–ALIX regulates the biogenesis of exosomes. *Nature Cell Biology*, *14*, 677–685.

Bebelman, M. P., Bun, P., Huveneers, S., Van Niel, G., Pegtel, D. M., & Verweij, F. J. (2020). Real-time imaging of multivesicular body-plasma membrane fusion to quantify exosome release from single cells. *Nature Protocols*, *15*, 102–121.

Bobrie, A., Colombo, M., Raposo, G., & Théry, C. (2011). Exosome secretion: Molecular mechanisms and roles in immune responses. *Traffic (Copenhagen, Denmark)*, *12*, 1659–1668.

Böing, A. N., Van Der Pol, E., Grootemaat, A. E., Coumans, F. A. W., Sturk, A., & Nieuwland, R. (2014). Single-step isolation of extracellular vesicles by size-exclusion chromatography. *J Extracell Vesicles*, *3*, 23430.

Busatto, S., Vilanilam, G., Ticer, T., Lin, W.-L., Dickson, D., Shapiro, S., Bergese, P., & Wolfram, J. (2018). Tangential flow filtration for highly efficient concentration of extracellular vesicles from large volumes of fluid. *Cells*, *7*, 273.

Chevalier, R. L. (2016). The proximal tubule is the primary target of injury and progression of kidney disease: Role of the glomerulotubular junction. *American Journal of Physiology. Renal Physiology*, *311*, F145–F161.

Cijsouw, T., Ramsey, A., Lam, T., Carbone, B., Blanpied, T., & Biederer, T. (2018). Mapping the proteome of the synaptic cleft through proximity labeling reveals new cleft proteins. *Proteomes*, *6*, 48.

Cvjetkovic, A., Jang, S. C., Konečná, B., Höög, J. L., Sihlbom, C., Lässer, C., & Lötvall, J. (2016). Detailed analysis of protein topology of extracellular vesicles-evidence of unconventional membrane protein orientation. *Science Reports*, *6*, 36338.

Del Olmo, T., Lauzier, A., Normandin, C., Larcher, R., Lecours, M., Jean, D., Lessard, L., Steinberg, F., Boisvert, F.-M., & Jean, S. (2019). APEX2-mediated RAB proximity labeling identifies a role for RAB21 in clathrin-independent cargo sorting. *Embo Reports*, *20*, e47192.

Fazal, F. M., Han, S., Parker, K. R., Kaewsapsak, P., Xu, J., Boettiger, A. N., Chang, H. Y., & Ting, A. Y. (2019). Atlas of subcellular RNA localization revealed by APEX-seq. *Cell*, *178*, 473–490.e26.

Ghossoub, R., Lembo, F., Rubio, A., Gaillard, C. B., Bouchet, J., Vitale, N., Slavík, J., Machala, M., & Zimmermann, P. (2014). Syntenin-ALIX exosome biogenesis and budding into multivesicular bodies are controlled by ARF6 and PLD2. *Nature Communication*, *5*, 3477.

Hessvik, N. P., & Llorente, A. (2018). Current knowledge on exosome biogenesis and release. *Cellular and Molecular Life Sciences*, *75*, 193–208.

Jeppesen, D. K., Fenix, A. M., Franklin, J. L., Higginbotham, J. N., Zhang, Q., Zimmerman, L. J., Liebler, D. C., Ping, J., Liu, Qi., Evans, R., Fissell, W. H., Patton, J. G., Rome, L. H., Burnette, D. T., & Coffey, R. J. (2019). Reassessment of exosome composition. *Cell*, *177*, 428–445.e18.

Jeppesen, D. K., Hvam, M. L., Primdahl-Bengtson, B., Boysen, A. T., Whitehead, B., Dyrskjøt, L., Ørntoft, T. F., Howard, K. A., & Ostenfeld, M. S. (2014). Comparative analysis of discrete exosome fractions obtained by differential centrifugation. *Journal of Extracellular Vesicles*, *3*, 25011.

Keerthikumar, S., Chisanga, D., Ariyaratne, D., Al Saffar, H., Anand, S., Zhao, K., Samuel, M., Pathan, M., Jois, M., Chilamkurti, N., Gangoda, L., & Mathivanan, S. (2016). ExoCarta: A web-based compendium of exosomal cargo. *Journal of Molecular Biology*, *428*, 688–692.

Kolde, R., & Vilo, J. (2015). GOsummaries: An R package for visual functional annotation of experimental data. *F1000Res*, *4*, 574.

Kwon, S.-H., Liu, K. D., & Mostov, K. E. (2014). Intercellular transfer of GPRC5B via exosomes drives HGF-mediated outward growth. *Current Biology*, *24*, 199–204.

Lakkaraju, A., & Rodriguez-Boulan, E. (2008). Itinerant exosomes: Emerging roles in cell and tissue polarity. *Trends in Cell Biology*, *18*, 199–209.

Lam, S. S., Martell, J. D., Kamer, K. J., Deerinck, T. J., Ellisman, M. H., Mootha, V. K., & Ting, A. Y. (2015). Directed evolution of APEX2 for electron microscopy and proximity labeling. *Nature Methods*, *12*, 51–54.

Leidal, A. M., Huang, H. H., Marsh, T., Solvik, T., Zhang, D., Ye, J., Kai, F., Goldsmith, J., Liu, J. Y., Huang, Y.-H., Monkkonen, T., Vlahakis, A., Huang, E. J., Goodarzi, H., Yu, L., Wiita, A. P., & Debnath, J. (2020). The LC3-conjugation machinery specifies the loading of RNA-binding proteins into extracellular vesicles. *Nature Cell Biology*, *22*, 187–199.

Li, J., Liu, K., Liu, Y., Xu, Y., Zhang, F., Yang, H., Liu, J., Pan, T., Chen, J., Wu, M., Zhou, X., & Yuan, Z. (2013). Exosomes mediate the cell-to-cell transmission of IFN-alpha-induced antiviral activity. *Nature Immunology*, *14*, 793–803.

Lobingier, B. T., Hüttenhain, R., Eichel, K., Miller, K. B., Ting, A. Y., Von Zastrow, M., & Krogan, N. J. (2017). An approach to spatiotemporally resolve protein interaction networks in living cells. *Cell*, *169*, 350–360.e12.

Loh, K. H., Stawski, P. S., Draycott, A. S., Udeshi, N. D., Lehrman, E. K., Wilton, D. K., Svinkina, T., Deerinck, T. J., Ellisman, M. H., Stevens, B., & Carr, S. A., Ting, A. Y. (2016). Proteomic analysis of unbounded cellular compartments: Synaptic clefts. *Cell*, *166*, 1295–1307.e21.

Ma, Z., Li, L., Livingston, M. J., Zhang, D., Mi, Q., Zhang, M., Ding, H.-F., Huo, Y., Mei, C., & Dong, Z. (2020). p53/microRNA-214/ULK1 axis impairs renal tubular autophagy in diabetic kidney disease. *Journal of Clinical Investigation*, *130*, 5011–5026.

Martell, J. D., Deerinck, T. J., Lam, S. S., Ellisman, M. H., & Ting, A. Y. (2017). Electron microscopy using the genetically encoded APEX2 tag in cultured mammalian cells. *Nature Protocols*, *12*, 1792–1816.

Martell, J. D., Deerinck, T. J., Sancak, Y., Poulos, T. L., Mootha, V. K., Sosinsky, G. E., Ellisman, M. H., & Ting, A. Y. (2012). Engineered ascorbate peroxidase as a genetically encoded reporter for electron microscopy. *Nature Biotechnology*, *30*, 1143–1148.

Melo, S. A., Sugimoto, H., O'connell, J. T., Kato, N., Villanueva, A., Vidal, A., Qiu, L., Vitkin, E., Perelman, L. T., Melo, C. A., Lucci, A., Ivan, C., Calin, G. A., & Kalluri, R. (2014). Cancer exosomes perform cell-independent microRNA biogenesis and promote tumorigenesis. *Cancer Cell*, *26*, 707–721.

Momen-Heravi, F., Balaj, L., Alian, S., Trachtenberg, A. J., Hochberg, F. H., Skog, J., & Kuo, W. P. (2012). Impact of biofluid viscosity on size and sedimentation efficiency of the isolated microvesicles. *Frontiers in Physiology*, *3*, 162.

Pastuzyn, E. D., Day, C. E., Kearns, R. B., Kyrke-Smith, M., Taibi, A. V., Mccormick, J., Yoder, N., Belnap, D. M., Erlendsson, S., Morado, D. R., Briggs, J. A. G., Feschotte, C., & Shepherd, J. D. (2018). The neuronal gene arc encodes a repurposed retrotransposon gag protein that mediates intercellular RNA transfer. *Cell*, *172*, 275–288.e18.

Poeter, M., Brandherm, I., Rossaint, J., Rosso, G., Shahin, V., Skryabin, B. V., Zarbock, A., Gerke, V., & Rescher, U. (2014). Annexin A8 controls leukocyte recruitment to activated endothelial cells via cell surface delivery of CD63. *Nature Communication*, *5*, 3738.

Ramanathan, M., Majzoub, K., Rao, D. S., Neela, P. H., Zarnegar, B. J., Mondal, S., Roth, J. G., Gai, H., Kovalski, J. R., Siprashvili, Z., Palmer, T. D., Carette, J. E., & Khavari, P. A. (2018). RNA-protein interaction detection in living cells. *Nature Methods*, *15*, 207–212.

Ratliff, B. B., Abdulmahdi, W., Pawar, R., & Wolin, M. S. (2016). Oxidant mechanisms in renal injury and disease. *Antioxidants & Redox Signaling*, *25*, 119–146.

Rider, M. A., Cheerathodi, M. R., Hurwitz, S. N., Nkosi, D., Howell, L. A., Tremblay, D. C., Liu, X., Zhu, F., & Meckes, D. G. (2018). The interactome of EBV LMP1 evaluated by proximity-based BioID approach. *Virology*, *516*, 55–70.

Ritchie, M. E., Phipson, B., Wu, Di., Hu, Y., Law, C. W., Shi, W., & Smyth, G. K. (2015). limma powers differential expression analyses for RNA-sequencing and microarray studies. *Nucleic Acids Research*, *43*, e47.

Schöneberg, J., Lee, I.-H., Iwasa, J. H., & Hurley, J. H. (2017). Reverse-topology membrane scission by the ESCRT proteins. *Nature Reviews Molecular Cell Biology*, *18*, 5–17.

Shah, R., Patel, T., & Freedman, J. E. (2018). Circulating extracellular vesicles in human disease. *New England Journal of Medicine*, *379*, 958–966.

Shurtleff, M. J., Temoche-Diaz, M. M., Karfilis, K. V., Ri, S., & Schekman, R. (2016). Y-box protein 1 is required to sort microRNAs into exosomes in cells and in a cell-free reaction. *Elife*, *5*, e19276.

Takahashi, K., Avissar, N., Whitin, J., & Cohen, H. (1987). Purification and characterization of human plasma glutathione peroxidase: A selenoglycoprotein distinct from the known cellular enzyme. *Archives of Biochemistry and Biophysics*, *256*, 677–686.

Tosar, J. P., Segovia, M., Castellano, M., Gámbaro, F., Akiyama, Y., Fagúndez, P., Olivera, Á., Costa, B., Possi, T., Hill, M., Ivanov, P., & Cayota, A. (2020). Fragmentation of extracellular ribosomes and tRNAs shapes the extracellular RNAome. *Nucleic Acids Research*, *48*, 12874–12888.

Wethmar, K. (2014). The regulatory potential of upstream open reading frames in eukaryotic gene expression. *Wiley Interdisciplinary Reviews RNA*, *5*, 765–768.

Wilson, J. M., De Hoop, M., Zorzi, N., Toh, B.-H., Dotti, C. G., & Parton, R. G. (2000). EEA1, a tethering protein of the early sorting endosome, shows a polarized distribution in hippocampal neurons, epithelial cells, and fibroblasts. *Molecular Biology of the Cell*, *11*, 2657–2671.

Yim, N., Ryu, S.-W., Choi, K., Lee, K. R., Lee, S., Choi, H., Kim, J., Shaker, M. R., Sun, W., Park, J.-H., Kim, D., Heo, W. D., & Choi, C. (2016). Exosome engineering for efficient intracellular delivery of soluble proteins using optically reversible protein-protein interaction module. *Nature Communication*, *7*, 12277.

Yuana, Y., Levels, J., Grootemaat, A., Sturk, A., & Nieuwland, R. (2014). Co-isolation of extracellular vesicles and high-density lipoproteins using density gradient ultracentrifugation. *Journal of Extracellular Vesicles*, *3*, 23262.

Zhang, H., Freitas, D., Kim, H. S., Fabijanic, K., Li, Z., Chen, H., Mark, M. T., Molina, H., Martin, A. B., Bojmar, L., Fang, J., Rampersaud, S., Hoshino, A., Matei, I., Kenific, C. M., Nakajima, M., Mutvei, A. P., Sansone, P., Buehring, W., & …, Lyden, D. (2018). Identification of distinct nanoparticles and subsets of extracellular vesicles by asymmetric flow field-flow fractionation. *Nature Cell Biology*, *20*, 332–343.

Zhang, M., & Schekman, R. (2013). Cell biology. Unconventional secretion, unconventional solutions. *Science*, *340*, 559–561.

SUPPORTING INFORMATION

Additional supporting information can be found online in the Supporting Information section at the end of this article.

How to cite this article: Lee, B. R., Lee, T. J., Oh, S., Li, C., Song, J.-H. A., Marshall, B., Zhi, W., & Kwon, S.-H. (2022). Ascorbate peroxidase-mediated in situ labeling of proteins in secreted exosomes. *Journal of Extracellular Vesicles*, *11*, e12239. https://doi.org/10.1002/jev2.12239